

**DISSIPATION INSIDE MARS AT TIDAL AND SEISMIC FREQUENCIES.** F. Nimmo, *Dept. Earth & Planetary Sciences, U.C. Santa Cruz, Santa Cruz CA, USA (fnimmo@es.ucsc.edu)*, U.H. Faul, *Dept. Earth Atmospheric & Planetary Sciences, MIT, Cambridge MA, USA (ufaul@bu.edu)*.

**Introduction** The rate at which tidal energy is dissipated within solid bodies can be measured, and provides constraints on the interior properties of those bodies. Dissipation is often quantified by a tidal quality factor  $Q$ , where large  $Q$  means small dissipation. The tidal- $Q$  factors of Mars and the solid Earth are  $85.6 \pm 0.4$  [1] and  $90$  [2] at periods of roughly 7 and 300 hours, respectively. On the face of it, this is a surprising result - the shorter period at Mars should produce a higher  $Q$  than Earth. Furthermore, application of simple (Maxwell) viscoelastic dissipation models to the case of Mars [1] require mantle viscosities that are several orders of magnitude smaller than expected values. Below we show that the use of a dissipation model based on laboratory experiments resolves this paradox, and produces the correct Martian  $Q$  for reasonable interior structure models [cf. 3]. Because  $Q$  is highly sensitive to temperature, we estimate a Martian mantle potential temperature  $\approx 1450$  K for a grain-size of 1 mm. We also predict a low-velocity zone at the base of the Martian lithosphere [cf. 4], relevant to the INSIGHT mission [5].

**Observations** The astrometrically-measured inwards drift of Phobos due to dissipation in Mars has been used to infer the Martian value of  $k_2/Q$  at the period of Phobos (7.65 h) [1]. The response of Mars to solar tides has been used to infer  $k_2 = 0.163 \pm 0.056$  at the annual period (1.88 yr) [1,6]. Secondary observational constraints include the moment of inertia ( $C/MR^2 = 0.365$ ), inferred from the observed precession of the Martian rotation pole [6] and the inferred elastic thickness of the Martian lithosphere. This latter quantity may exceed 300 km at the north pole [7] and is roughly 80 km for Amazonian-age features [8].

**Model** Our model approach is almost identical to that of [9]. The only difference is in our calculation of mantle temperature structure, which for Mars is convective. In the lithosphere we take the potential temperature  $T_p$  to be given by

$$T_p(z) = T_s + \frac{(T_m - T_s)z}{L} \quad (1)$$

Here  $T_s$  is the surface temperature,  $T_m$  is the potential temperature of the convecting interior,  $L$  is the thickness of the conductive stagnant lid and depth  $z = R - r$  where  $R$  is the radius of Mars. In general, the stagnant lid thickness is expected to be larger (by a factor of  $\approx 2$ ) than the elastic thickness.

To convert from potential temperature to actual temperature  $T(z)$  we multiply  $T_p(z)$  by an adiabatic factor  $f_{ad}$ . The adiabatic temperature gradient  $dT/dz = \alpha g T / C_p$ , where  $\alpha$  and  $C_p$  are thermal expansivity and specific heat capacity, respectively, and  $g(r)$  is the acceleration due to gravity. Taking  $\alpha$  and  $C_p$  to be constant, we find

$$\ln f_{ad} = \frac{4}{3} \frac{G\alpha}{C_p} \left[ -\frac{R_c^3}{R} \Delta\rho \frac{z/R}{1-(z/R)} + \rho_m \left( Rz - \frac{z^2}{2} \right) \right] \quad (2)$$

where  $G$  is the gravitational constant,  $R_c$  is the core radius,  $\rho_m$  is the mean mantle density and  $\Delta\rho$  is the core-mantle density contrast.

Our model is deliberately highly simplified to allow efficient exploration of parameter space, and because neither  $Q$  nor  $k_2$  are likely to be significantly affected by secondary phases. Dissipation is calculated using the same approach as [9]. The complex shear modulus as a function of depth is calculated using the extended Burgers rheology of [10], assuming dry, melt-free, polycrystalline  $Fo_{90}$  olivine. The bulk quantities  $k_2$  and  $Q$  are then obtained using the method of [11], assuming a liquid core [6].

**Results** Fig 1 plots the result of our nominal model, for which  $L=300$  km,  $T_m=1463$  K and the grain size is 1 mm. Fig 1a shows the present-day mean mantle temperature structure compared with a suite of convection models from [12]. Our simplified structure reproduces the basic characteristics of these numerical models, which have a lid thickness in the range 300-500 km. Note the steep temperature gradient in the lithosphere, an effect not included in some earlier petrological models of the Martian interior [13-15]. Fig 1b plots the model density structure compared with experimentally-determined values [16]. The overall trend is well matched, although our simplified model does not include the phase changes likely present in the real mantle. The viscosity (not shown) is strongly depth-dependent, with a minimum of about  $10^{22}$  Pa s at the base of the lithosphere.

Fig 1c likewise compares our model shear velocity with predicted shear wave velocities from several studies [15]. Our model does not include the jump in  $V_s$  at mid-mantle depths due to the phase change. More importantly, we predict a low velocity zone at the base of the lithosphere [cf. 4]. This LVZ arises because of the competing effects of temperature and pressure on rigidity. The LVZ is more pronounced than on the Earth, because on Mars the temperature gradient in the lithosphere is about the same, but the pressure gradient is three times smaller than on Earth. Such an LVZ is potentially detectable using normal modes or surface wave dispersion. The LVZ at the base of the mantle is not predicted in some other studies because they assume near-surface temperatures that are too warm [13].

Finally, Fig 1d plots  $Q$  as a function of depth at both seismic and tidal frequencies. The  $Q$  in the lid is very large (little dissipation) because of the cold temperatures involved. The actual  $Q$  is likely to be smaller, because of scattering in the near-surface (an effect not modelled here). The seismic  $Q$  in the convecting mantle is approximately constant,  $Q \approx 130$ . The tidal  $Q$  is lowest (most dissipative) in the upper mantle; thus, our neglect of deeper mantle phase changes is unlikely to affect the results. For this model, the bulk  $Q$  at Phobos' period is 87 and the  $k_2$  at annual period is 0.161, in agreement with the observations.

## DISSIPATION IN MARS: F. Nimmo, U.H. Faul

Figure 2 plots how  $k_2$  and  $Q$  vary as the lid thickness  $L$  and mantle potential temperature  $T_m$  are varied. Fig 2a shows that increasing  $T_m$  increases dissipation (decreases  $Q$ ), as expected, while a thicker lid reduces dissipation. Similarly, in Fig 2b a thicker lid reduces  $k_2$ , as expected, while increasing  $T_m$  increases  $k_2$ , because a warmer planet is more deformable. However, the uncertainties in  $k_2$  are sufficiently large that it does not provide a useful constraint.

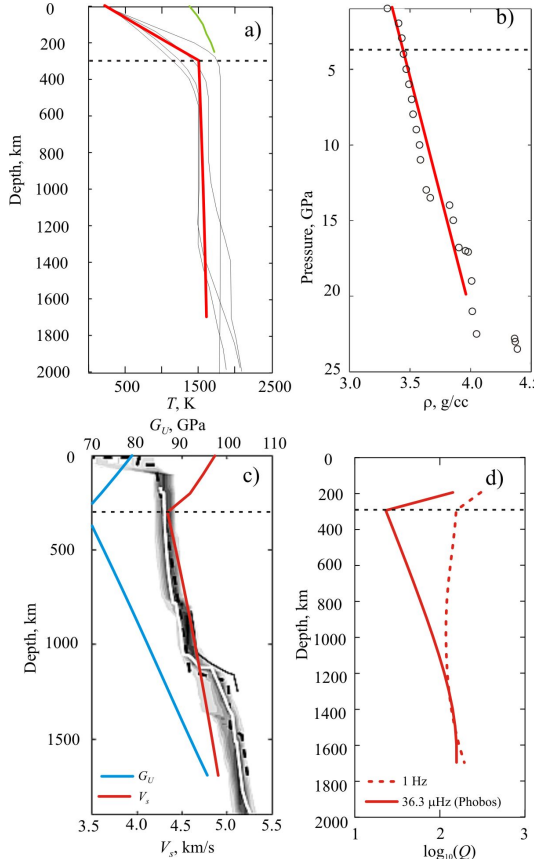


Figure 1: a) Model temperature (red line; equations 1 and 2) compared with a suite of numerical convection models [12] (black lines). Green line is a model Martian solidus [18]. Dashed line indicates base of lithosphere. b) Model density as a function of pressure (solid line), compared with experimentally-determined densities [16]. c) Model shear wave velocity  $V_s$  (red line) compared with several petrological models [15]. Note the low velocity zone at the base of the lithosphere. Blue line is unrelaxed shear modulus  $G_U$ . d) Dissipation factor  $Q$  at tidal and seismic frequencies with  $d=1$  mm.

The red line in Fig 2a shows the estimated  $Q$  for Mars, and the white star denotes our nominal model (Fig 1). There is evidently a tradeoff between  $L$  and  $T_m$ : a thicker lid requires a hotter mantle (but a lower heat flux) to match the observed  $Q$ . The sensitivity to lid thickness is not very great: varying  $L$  from 50 to 500 km results in a mantle potential temperature

range of 1440–1510 K. The nominal model yields a heat flux of  $13 \text{ mW m}^{-2}$ . This value is significantly less than the likely radiogenic rate of  $\approx 20 \text{ mW m}^{-2}$  [12] (though note that these elements may be concentrated in the crust) and suggests that our nominal value of  $T_m$  is conservatively high.

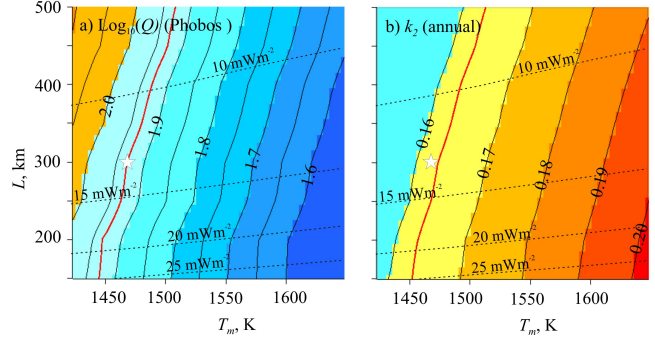


Figure 2: a) Variation of bulk  $Q$  as a function of mantle potential temperature  $T_m$  and lid thickness  $L$ . Star indicates our nominal model (Fig 1), red line indicates measured  $Q$  value and dashed lines give heat flux. b) As for a), except for  $k_2$ .

**Discussion** Probably the biggest uncertainty in our calculations of  $Q$  is the grain size  $d$ . Increasing  $d$  requires higher temperatures to deliver the same  $Q$ . For instance, taking  $d=1$  cm and a lid thickness of 300 km, a potential temperature of  $T_m = 1610$  K is required to match the  $Q$  of Mars (an increase of almost 150 K over the  $d=1$  mm case).

One possible way of reducing the uncertainty in  $T_m$  is to consider melting. Higher values of  $T_m$  result in greater melt production at the present day; detailed modelling [11,17] is beyond the scope of this analysis but favours the  $d=1$  cm case (high  $T_m$ ). On the other hand, the implied viscosities in this case are so large (because of the larger  $d$ ) that convection is not assured. Finally, because dissipation is strongly increased in the presence of melt or water, a lower  $T_m$  will be required to match the observations if water or melt are present. Electrical conductivity measurements [4] may provide one way of resolving this issue.

## References

- [1] Bills BG et al., JGR 110, E07004, 2005. [2] Ray RD, GD Egbert, GJI 189, 400–413, 2012. [3] Castillo JC, WB Banerdt, Mantle of Mars workshop, 6032, 2012. [4] Mocquet A, M Menouille, PSS 48, 1249–1260, 2000. [5] Lognonne P et al., LPSC 43, 1983, 2012. [6] Yoder CF et al., Science 300, 299–303, 2003. [7] Phillips RJ et al., Science 320, 1182–1185, 2008. [8] McGovern PJ et al., JGR 109, E07007, 2004. [9] Nimmo F et al., JGR 117, E09005, 2012. [10] Jackson I, UH Faul, PEPI 183, 151–164, 2010. [11] Roberts JH, F Nimmo, Icarus 194, 675–689, 2008. [12] Ogawa M, T Yanagisawa, JGR 116, E08008, 2011. [13] Bertka CM, YW Fei, JGR 102, 5251–5264, 1997. [14] Gudkova TV, VN Zharkov, PEPI 142, 1–22, 2004. [15] Khan A, JAD Connolly, JGR 113, E07003, 2008. [16] Bertka CM, YW Fei, EPSL 157, 79, 1998. [17] Kiefer WS, MAPS 38, 1815–1832, 2003. [18] Bertka CM, JR Holloway, CMP 115, 313–322, 1994.